THREE-DIMENSIONAL SLOPE STABILITY METHODS IN GEOTECHNICAL PRACTICE

Timothy D. Stark[1], Member, ASCE

ABSTRACT

Study of several field case histories showed that the difference between two and three-dimensional factors of safety against slope failure is most pronounced in cases that involve a translational failure mode through low shear strength materials. Two and three-dimensional slope stability analyses of field case histories and a parametric study of a typical slope geometry revealed that commercially available three-dimensional slope stability programs have some limitations including: (1) accounting for the shearing resistance along the sides of a sliding mass, (2) modeling the failure envelopes of the materials involved, and (3) considering the internal forces in the slide mass. These limitations can affect the calculated factor of safety for a translational failure mode. A new technique is presented to overcome some of these limitations and provide a better estimation of the three-dimensional factor of safety. Field case histories are presented to illustrate the use of a three-dimensional analysis in back-calculating the mobilized shear strength of the materials involved in a slope failure for use in remedial measures and design of slopes with complicated topography, shear strength, and pore-water pressures.

INTRODUCTION

At present, most slope stability analyses are performed using a two-dimensional (2-D) limit equilibrium method. These methods calculate the factor of safety against failure for a slope assuming a plane-strain condition. Therefore, it is implicitly assumed that the slip surface is infinitely wide, and thus three-dimensional (3-D) effects are negligible because of the infinite width of the slide mass. Clearly, slopes are not infinitely wide and 3-D effects influence the stability of most, if not all, slopes. In general, the 2-D analysis is appropriate for slope design because it yields a conservative estimate for the factor of safety (Duncan 1992). It is conservative because the end effects are not included in the 2-D estimate of the factor of safety. A 3-D analysis is recommended for back-analysis of slope failures so that the back-calculated mobilized shear strength reflects the 3-D end effects. The 3-D back-calculated shear strength can be used in remedial measures for failed slopes or slope design in sites with similar conditions.

Skempton (1985) suggests applying the following three-dimensional correction factor to the shear strength back-calculated from a two-dimensional analysis:

$$\frac{1}{1+\dfrac{KD}{B}} \tag{1}$$

---

[1] Professor of Civil and Environmental Engrg., University of Illinois, 205 N. Mathews Ave., Urbana, IL, 61801-2352, (217) 333-7394, e-mail: t-stark1@uiuc.edu

where K is the coefficient of earth pressure mobilized at failure, D is the average depth of the failure mass, and B is the average width of the failure mass. Skempton (1985) also reports that this correction factor usually results in a 5% increase in the back-calculated shear strength. However, this 5% correction is an average value, and varies for different cases and material types. It will be shown herein that the percentage can be as large as 30% and thus a three-dimensional analysis should be conducted to back-calculate shear strengths from a known failure surface.

A number of 3-D slope stability methods and computer programs have been developed. The validity of the analytical results depends on the degree to which the analysis matches the field mechanics and the success of the user in modeling the field geometry and engineering properties with the program. Most of the existing 3-D slope stability methods and computer programs have been evaluated using parametric studies and not field case histories, e.g., Chen and Chameau (1983), Lovell (1984), and Thomaz and Lovell (1988). Therefore, a widely accepted 3-D stability analysis is not yet available for practicing geotechnical engineers. Through analysis of field case histories, this paper introduces the site conditions in which a 3-D stability analysis is most important, investigates the accuracy of available 3-D stability methods and software, presents a technique to improve this accuracy, and finally provides a comparison of 2-D and 3-D analyses.

FAILURE MODE FOR 3-D SLOPE STABILITY STUDY

To achieve the above objectives, case histories that involve *translational failure* through a weak material, such as *cohesive and/or geosynthetic materials* were studied. This type of failure was chosen for the following reasons:

1.) Slopes failing in translational mode usually involve either a significantly higher or lower mobilized shear strength along the back scarp and sides of the slide mass than that along the base, e.g. upstream slope failure in Waco dam (Beene 1967; Wright and Duncan 1972) and slope failure in Kettleman Hills hazardous waste repository (Seed et al 1990; Byrne et al. 1992; and Stark and Poeppel 1994), respectively. These situations can result in a significant difference between the 2-D and 3-D factors of safety. This difference is less pronounced in slopes failing in rotational mode which usually occurs in homogenous materials (Figure 1).
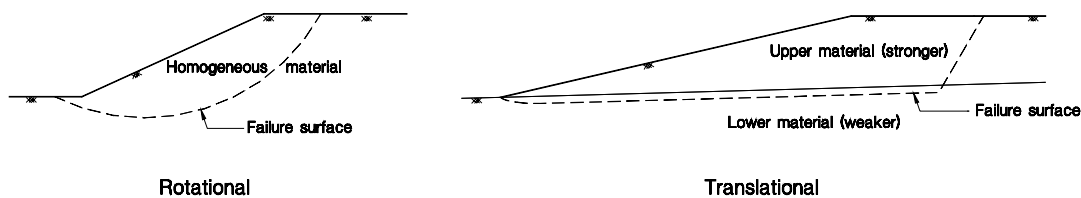

Figure 1. Two Different Failure Modes for Slopes.

2.) A translational failure likely occurs in relatively flat slopes. The flatter the slope, the greater the difference between 2-D and 3-D factors of safety (Chen and Chameau 1983; Leshchinsky et al. 1985).

3.) A translational failure often involves a long and nearly horizontal sliding base through a pre-existing failure surface along which a residual shear strength condition is mobilized in soils, e.g. Maymont slide (Krahn et al. 1979), Gardiner Dam movement (Jasper and Peters 1979), and Portuguese Bend slide (Ehlig 1992). If geosynthetics are involved, a translational failure mode may occur without mobilizing a post-peak shear strength condition because of the low peak strength of some geosynthetic interfaces. The presence of a pre-existing failure surface or weak interface in these cases can provide some certainty in the shear strength input data. In contrast, a rotational failure in homogeneous material usually involves a progressive failure mechanism which may lead to a poor estimation of the mobilized shear strength (Eid 1996).

4.) A translational failure often involves a drained shearing condition. This facilitates estimation of the mobilized shear strength of the materials involved.

5.) A three-dimensional stability analysis is generally needed for a failed slope to estimate the mobilized shear strength of the involved materials for use in remedial measures or design of slopes at sites with similar geotechnical characteristics. This is most common after a translational failure.

6.) The end effects are more pronounced for slopes of cohesive materials (Chen 1981; Lovell 1984; Leshchinsky and Baker 1986; Ugai 1988).

THREE-DIMENSIONAL SLOPE STABILITY SOFTWARE

Commercially available 3-D slope stability software was studied to investigate the ability of the software to calculate an accurate 3-D factor of safety. The studied software includes 3D-PCSTABL (Thomaz 1986), CLARA 2.31 (Hunger 1988), and TSLOPE3 (Pyke 1991). The following 3-D stability software was also investigated but the limitation of a 3-D shear surface with only a cylindrical shape precluded their use in the study: STAB3D (Baligh and Azzouz 1975), LEMIX&FESPON (Chen and Chameau 1983), BLOCK3 (Lovell 1984), and F3SLOR&DEEPCYL (Gens et al. 1988). Several case histories were analyzed using 3D-PCSTABL, CLARA 2.31, and TSLOPE3 to study the effect of the capabilities and limitations in describing the slope geometry and pore-water pressure conditions, modeling the material shear strength behavior, and calculating the minimum 3-D and 2-D factors of safety. Table 1 gives a brief description of the main differences between these programs for analyzing the translational failure mode.

Table 1. Main Differences between Commerically Available 3D Slope Stability Software for Analyzing Translational Slope Failures.

Program name (1)	Theoretical basis for 3D method (2)	Statical assumptions (3)	Equilibrium condition satisfied (4)	Shape of failure surface (5)	Piezometric pressure specification (6)	Number of possible piezometric surfaces (7)	Shear strength Models (8)	Calculating Yield Seismic coefficient (9)	Accommodating external loads (10)	Search for direction of minimum FS for certain failure mass (11)	Search for 3D critical failure surface (12)	2D analysis out of 3D data file (13)	Creating Data File (14)
CLARA 2.31 (Hungr 1988)	Bishop's simplified method or Janbu's simplified method	Vertical inter-column and moment	Vertical force and moment	Any	Hydro-static or using pore-pressure ratio "r_u"	Several	Linear Mohr-Coulomb envelope or para-bolic -envelope [proposed by Hoek and Brown (1980)]	Yes	Yes	Yes	Yes (for circular surface only)	Yes	Using an inter-action inter-face
TSLOPE3 (Pyke 1991)	Los Angeles County method	Inter-column forces are zero	Horizontal force	Any	Hydro-static	One	Linear or non-linear Mohr-Coulomb enve-lope or para-bolic envelope [proposed by Hoek and Brown (1980)]	Yes	No	Yes	No	Yes	Using an editor or word processor
3D-PCSTABL (Thomaz 1986)	Method of slices	Interslice forces on the sides of the column have the same inclination; inter-column shear forces are parallel to the column base	All forces and moments	Symmetrical	Hydro-static or using pore-pressure ratio "r_u"	Several	Linear Mohr-Coulomb envelope	Yes	No	No	Yes	No	Using routine inter-face or word processor

As shown in Table 1, 3D-PCSTABL can only be used in the analysis of slopes with a symmetrical failure surface. This limitation prevents use of this software for most translational failures because the failure surface is usually asymmetrical in both horizontal and vertical directions. CLARA 2.31 and TSLOPE3 can analyze slopes with any shape of failure surface. However, CLARA 2.31 satisfies more conditions of equilibrium, utilizes different methods of 3-D analysis, and is more user-friendly than TSLOPE3. In addition, CLARA 2.31 has more capability in describing piezometric surfaces and external loads. As a result, CLARA 2.31 was used for all 3-D and some 2-D stability analyses described in this paper. It should be noted that all of the available 3-D slope stability software assumes that the whole sliding mass moves in the same direction, i.e., the direction of sliding is uniform for the entire mass. Consequently, this assumption was also applied to the 3-D stability analyses described in this paper.

CLARA 2.31 utilizes either an extension of Bishop's simplified method or Janbu's simplified method to three dimensions (Hungr 1987). The assumptions required to render the 3-D analysis statically determinate are the same as for the 2-D methods (Bishop 1955, and Janbu et al. 1968). Extending Bishop's simplified method, the intercolumn shear forces are assumed to be negligible and the vertical force equilibrium of each column and the overall moment equilibrium of the column assembly are sufficient conditions to determine all of the unknowns. Horizontal force equilibrium in both the longitudinal and transverse directions is neglected. The factor of safety equation is derived from the sum of moments around a common horizontal axis parallel to the x-direction. Janbu's simplified method assumes that conditions of horizontal and vertical force equilibrium are sufficient to determine all unknowns, and therefore, moment equilibrium is not satisfied. The factor of safety equation is derived from the horizontal force equilibrium equation. Figure 2 shows the forces acting on a typical column used in CLARA 2.31.
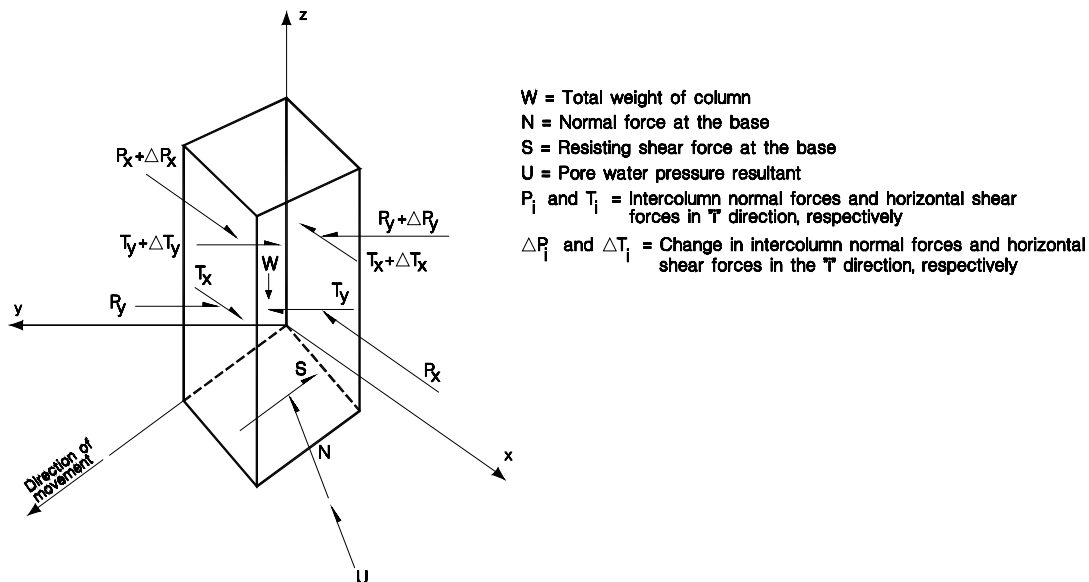

W = Total weight of column
N = Normal force at the base
S = Resisting shear force at the base
U = Pore water pressure resultant
P_i and T_i = Intercolumn normal forces and horizontal shear forces in 'i' direction, respectively
$\triangle P_i$ and $\triangle T_i$ = Change in intercolumn normal forces and horizontal shear forces in the 'i' direction, respectively

Figure 2. Forces Acting on Single Column [after Hungr (1987)]

PARAMETRIC STUDY

Limitations in describing the slope geometry and material properties and/or limitations in the analysis methods can result in poor estimates of the 3-D factor of safety using commercially available software. The effects of these limitations on the calculated 3-D factor of safety were studied using a model of a typical translational failure. A number of field case histories that experienced a translational failure mode were used to design the slope model so that it simulates field conditions with respect to slide mass dimensions (ratio between average depth and width), ground surface, side, and base slope inclinations, and material unit weights and shear strengths. Figure 3 shows a plan view and a representative cross section of this model.
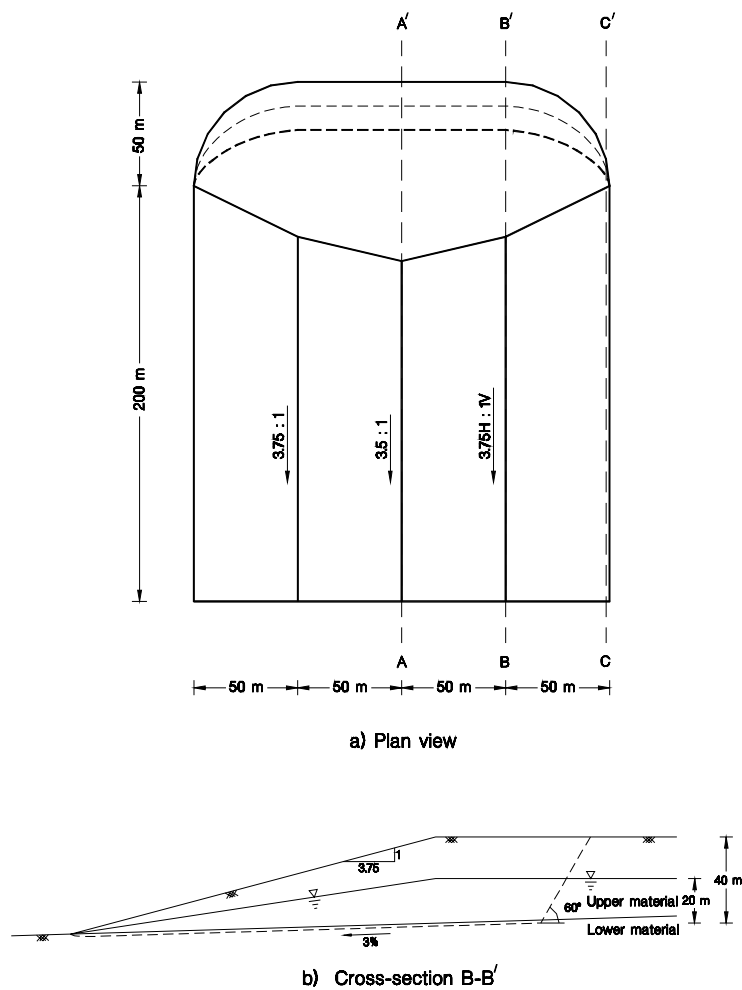
Figure 3. Plan View and Representative Cross Section for Slope Model: (a) Plan View; (b) Cross Section B-B′

Figure 4 shows the assumed failure envelopes of the two materials involved in the slope model analysis. The ratio in shear strength between the upper and lower materials is taken to simulate the ratio between the peak shear strength of a stiff fissured clay mass, i.e., the fully softened shear strength, and the residual shear strength of the same clay, respectively (Stark and Eid 1997). A liquid limit and clay size fraction of 95 percent and 50 percent, respectively, were assumed and used to estimate the shear strength values (Stark and Eid 1994, 1997). This shear strength ratio can also approximately simulate the ratio between the peak shear strength of municipal solid waste (Kavazanjian et al. 1995, and Stark et al. 1998) and the residual shear strength of a geosynthetic interface in the underlying composite liner system in a landfill (Stark et al. 1996). The saturated unit weights of the upper and lower materials were assumed to be 17 and 18 kN/m^3, respectively. Figure 4 also shows two linear approximations of the failure envelopes. Linear failure envelopes passing through the origin and the shear strength corresponding to the average normal stress on the slip surfaces yield friction angles of 23 and 8 degrees for the upper and lower materials, respectively. The effect of using this approximation and the actual failure envelope on the calculated 3-D factor of safety is discussed in a subsequent section of this paper.

It should be noted that the sides of the slide mass in the slope model are vertical. In translational failures, vertical sides provide the minimum amount of shear resistance because the effective normal stress acting on these sides is only due to the lateral earth pressure and a vertical side produces the minimum shear surface area. A translational failure with inclined sides usually occurs if inclined weak surfaces are present along the sides of the slide mass. This was the case in the slope failure at the Kettleman Hills hazardous waste repository.

The slope stability software divides the slide mass up into vertical columns. The user selects a grid spacing which is used to place a grid over the basal surface and to define the vertical columns into which the potential sliding mass is subdivided for the analysis. These columns are the 3-D equivalent of the vertical slices used in a
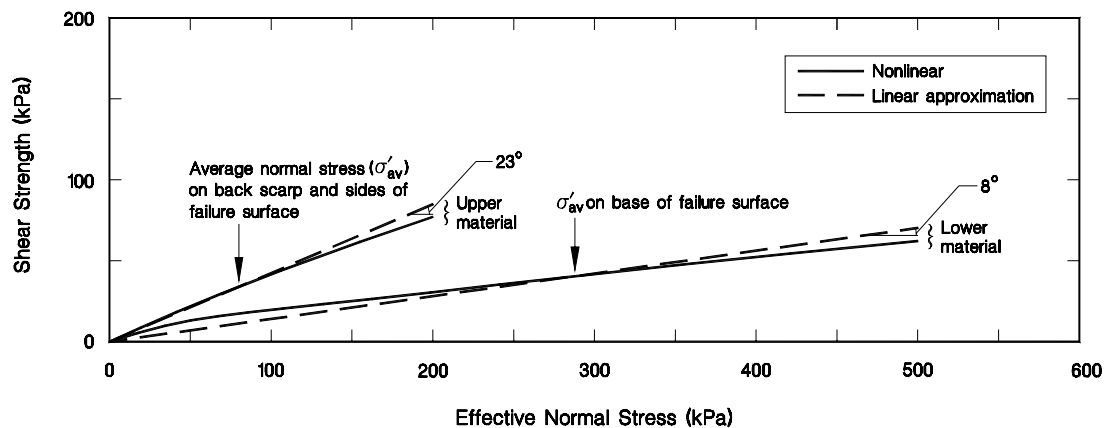
Figure 4. Shear Strength Envelopes Used for 3D Slope Model Analyses.
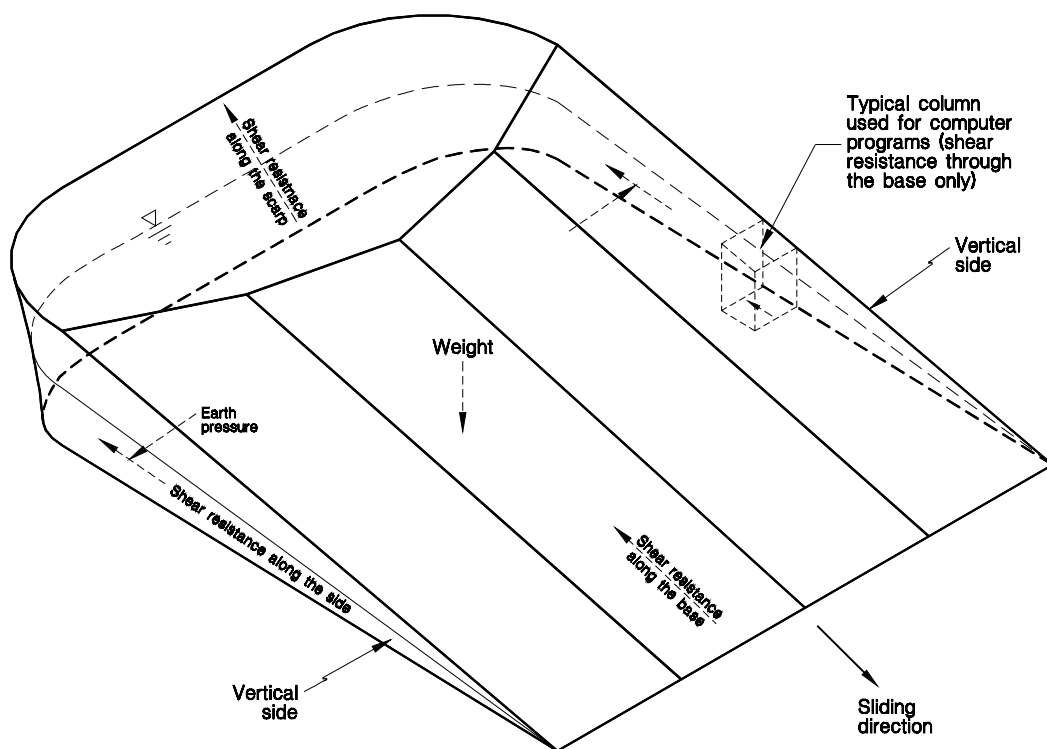
Figure 5. 3D View of Slope Model.

conventional 2-D analysis. The resisting forces are calculated by considering the material shear strength along the base of each column. As a result, the shear resistance due to cohesion and/or friction generated by the earth pressure on the sides of the vertical columns along the vertical sides of the slide mass is ignored (Figure 5). This usually leads to an underestimation of the 3-D factor of safety especially when the material along the vertical sides has a higher shear strength than the material along the base of the slide mass. An example of this situation is a failure surface that extends through municipal solid waste to an underlying a weak geosynthetic interface in the liner system.

Two and three-dimensional analyses were performed for the slope model to study the effect of ignoring the shear resistance along the vertical sides, using a linear approximation for a nonlinear failure envelope of the materials involved, and using different slope stability methods or assumptions on the calculated 3-D factor of safety. Table 2 shows the calculated 2-D and 3-D factors of safety for various analysis conditions. It should be noted that while CLARA 2.31 was used for the 3-D analyses, both the CLARA 2.31 and UTEXAS3 (Wright 1992) slope stability programs were used to calculate the 2-D factors of safety. UTEXAS3 was mainly used to incorporate a nonlinear failure envelope in the 2-D analysis by inputting a series of shear and normal stresses to describe the failure envelope.

Table 2. Factors of Safety for Model of Translational Failure.

Analysis type (1)	Input data (2)	Method of Analysis		
		Bishop (3)	Janbu (uncorrected) (4)	Spencer (5)
3D (using CLARA 2.31)	Ignoring side resistance	0.900	0.888	N/A
3D (using CLARA 2.31)	Considering side resistance	1.014	1.001	N/A
2D (using CLARA 2.31)	Section A-A′[a]	0.924	0.911	0.987
2D (using CLARA 2.31)	Section B-B′[a]	0.905	0.893	0.966
2D (using CLARA 2.31)	Section C-C′[a]	0.870	0.859	0.929
2D (using UTEXAS3)	Section A-A′[a]	N/A	N/A	0.987 (0.909)[b]
2D (using UTEXAS3)	Section B-B′[a]	N/A	N/A	0.966 (0.890)[b]
2D (using UTEXAS3)	Section C-C′[a]	N/A	N/A	0.929 (0.856)[b]

Note: N/A = not available
[a] Section location is shown in Figure 3.
[b] Nonlinear failure envelope was used.

Effect of Shearing Resistance along Vertical Sides of Slide Mass

As described previously, the available 3-D stability software does not consider the shearing resistance along the vertical sides of the sliding mass in calculating the 3-D factor of safety. To include this side resistance, a change in the input data was made so that a shearing force equivalent to the side resistance is used in calculating the 3-D factor of safety. This was accomplished for the slope model by using an "imaginary" material layer that surrounds only the sides of the slide mass. As a result, the material properties of this layer affect only the shear strength along the vertical sides and not the back scarp or base of the sliding mass. This layer has a unit weight equal to that of the upper material, a friction angle, ϕ'_i, of zero, and cohesion, c_i', equal to the shear strength due to the at-rest earth pressure acting on the vertical sides of the slide mass. The cohesion can be estimated using the following equation:

$$c_i' = k_o \sigma'_v \tan \phi' \qquad (2)$$

where σ'_v is the average vertical effective stress over the depth of the sliding mass side, ϕ' is the secant friction angle of the upper material corresponding to the approximated average effective normal stress on the vertical sides of the sliding mass, and k_o is the coefficient of earth pressure at rest for the upper layer material ($k_o = 1 - \sin \phi'$). In addition to using the imaginary layer, a slight (less than 5 degrees) outward inclination is assigned to each vertical side of the slide mass to include a single column so that the software can consider the effect of the cohesion in the shear resistance calculations. No resisting or driving force is mobilized due to the weight of this column because the friction angle of the imaginary layer is assumed to be zero.

9

The first two rows in Table 2 show that for the slope model considered herein, including the vertical side resistance increases the calculated 3-D factor of safety by about 13% using both Bishop's and Janbu's simplified methods. The side resistance effect should increase with increasing difference between the shear strength of the upper and lower layer. Table 2 also indicates that if the resistance along vertical sides is ignored, i.e., no side resistance, the calculated 3-D factor of safety is approximately equal to the average of the 2-D factors of safety through the slide mass.

Additional parametric studies were performed to investigate the effect of shear resistance along vertical sides as a function of slope angle. Figure 6 presents a relationship between the ratio of 3D/2D factors of safety (3D/2D FS) and the width/height (W/H) of the slide mass for the three slope inclinations considered. Two different slope heights of 10 and 100 m were also used but there was little, if any, difference between the factors of safety. For example, the 3D/2D FS ratio versus W/H results at H=10 and 100 m for the 1H:1V slope are the same. For the 3H:1V slope, the 3D/2D FS ratio versus W/H results at H=10 and 100 m are nearly the same with differences in 3D/2D FS ratios not exceeding 0.05. For the 5H:1V slope, the 3D/2D FS ratio versus W/H results at H=10 and 100 m differed by less than 0.06 for W/H values greater than 1.5. At a W/H ratio of 1, the 3D/2D FS ratio difference was 0.19. The slight differences in the 3D/2D FS ratio versus W/H results obtained at H = 10 and 100 m for the three slope inclinations is probably caused by the affects of CLARA 2.31 moving each input cross section so the x-coordinate coincides with the nearest row of column center points and the interpolation between these input cross sections which influences determination of 3D column parameters. In summary, slope heights of 10 and 100 m did not significantly affect the relationship between the ratio of 3D/2D factors of safety and W/H for the slope inclinations considered. This observation is in agreement with the concept of geometric similarity.
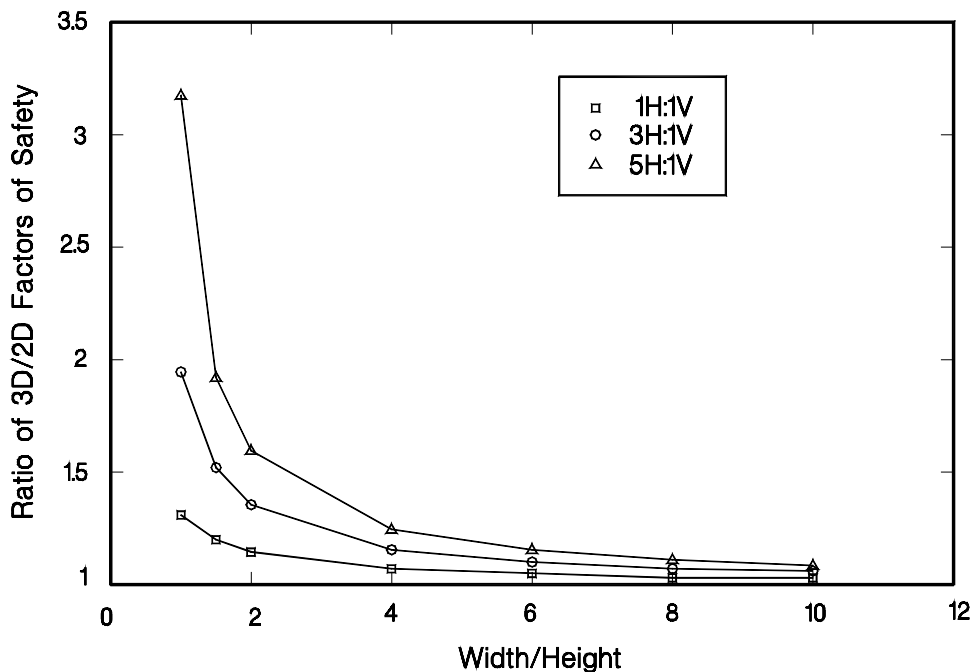

Figure 6. Effect of Shear Resistance along Vertical Sides of Slide Mass

The 3D factor of safety was greater than the 2D factor of safety for all of the W/H combinations used in the parametric study. It can be seen from Figure 6 that the 3D/2D FS ratio increases with decreasing W/H ratios for a given slope inclination. The area of the vertical, parallel sides of the slide mass are the same for a given slope inclination and height for all width values. As the width decreases, the weight of the slide mass decreases and the shearing resistance along the parallel sides has a greater effect on the 3D stability. This is evidenced in Figure 6 because the relationships increase rapidly at values of W/H less than 4. For W/H ratios less than 1.5, 3, and 5, the 3D factor of safety is at least 20 percent greater than the 2D factor of safety for the three slope inclinations. Therefore, the effect of including shearing resistance along the parallel sides of a slide mass increases as the slope width decreases.

Figure 6 also shows that as the slope inclination decreases, for a given W/H ratio, the 3D/2D FS ratio increases. This increase in 3D/2D FS ratio for a given W/H ratio results from an increase in the area of the vertical sides of the slide mass due to the increase in L with decreasing slope inclination. Therefore, the importance of incorporating end effects in a slope stability analysis increases with decreasing slope inclination. Chen and Chameau (1983) and Leshchinsky et al. (1985) also indicate that the flatter the slope, the greater the difference between 2D and 3D factors of safety. Therefore, in translational failures, which can occur in relatively flat slopes because of the presence of underlying weak material(s), the back-calculated shear strengths may be too high if end effects on the sides of the slide mass are ignored.

Importance of the Failure Envelope Nonlinearity

Nonlinear failure envelopes and their linear approximation shown in Figure 4 were used to calculate the 2-D factor of safety for different cross-sections of the slope model using Spencer's stability method (Spencer 1967). Each nonlinear failure envelope was modeled using 19 shear and normal stress combinations in UTEXAS3 (Wright 1992). Results in Table 2 show that ignoring the nonlinearity of the failure envelope, i.e., using a linear failure envelope that passes through the origin and the shear strength corresponding to the average normal stress on the slip surface, leads to an overestimation of the 2-D factors of safety by less than 10 percent. For example, ignoring the nonlinearity of the shear strength envelope in the analysis of cross section A-A increases the calculated 2-D factor of safety from 0.909 to 0.987. A similar effect is expected for the 3-D factor of safety but could not be verified because existing software doesn't allow a stress dependent failure envelope. The effect of ignoring the nonlinearity of the failure envelope should increase with an increase in the range of effective normal stress along the slip surface. As a result, it is recommended that 3-D slope stability software include an option for inputting a nonlinear failure envelope to account for stress-dependent shear strength.

Three-Dimensional Slope Stability Method

The slope stability methods differ in the statics employed in deriving the factor of safety equation and the assumptions used to render the limit equilibrium analysis

statically determinate. These differences affect the value of factor of safety calculated for each method. Quantitative comparisons of computed factors of safety have been made for a rotational failure mode by several researchers, e.g., Fredlund and Krahn (1977), Ching and Fredlund (1984) for 2-D stability analysis, and Leshchinsky and Baker (1986) for 3-D stability analysis. However, little information is available regarding the effect of the 3-D slope stability method on the calculated factor of safety for translational failures. This effect is presented in Table 2 using the 2-D results. The three different cross sections of the slope model were analyzed using Bishop's simplified, Janbu's simplified, and Spencer's methods.

Bishop's simplified method was originally derived for the rotational failures. It neglects vertical interslice forces and calculates the factor of safety based on moment equilibrium. Fredlund and Krahn (1977) extend the 2-D method by including moments of the normal forces and show satisfactory results for some non-rotational failure surfaces. Because the method neglects the internal shear strength in the vertical direction, Bishop's simplified method underestimates the factor of safety calculated using Spencer's method (Table 2). Janbu's simplified method assumes that the resultant interslice forces are horizontal and uses an empirical correction factor to account for the interslice vertical force. The factor of safety is calculated based on force equilibrium. If the correction factor is not used, Janbu's simplified method also underestimates the factor of safety calculated using Spencer's method. Spencer's method assumes that the resultant interslice forces have the same inclination throughout the sliding mass. Both force and moment equilibrium are satisfied in Spencer's method. This method is regarded as being accurate, i.e., within 6% of the correct 2-D factor of safety (Duncan 1992). This is especially true for the translational failure mode in which the inclination of the interslice force in the major part of the slope is almost constant.

Comparing the factors of safety calculated using these three stability methods presented in Table 2 shows that Bishop's and Janbu's simplified methods underestimate the factor of safety by approximately 6 and 8 percent, respectively, for the slope model. Underestimating the factor of safety increases with an increasing difference between the shear strength of the upper material, i.e., internal shear strength, and the shear strength along the sliding surface. A similar conclusion was reached by Hungr et al. (1989) for the effect of stability method on the calculated 2-D factor of safety.

For the slope model considered herein, overestimating the factor of safety due to ignoring the nonlinearity of the failure envelopes essentially cancels the underestimation of the factor of safety due to using Janbu's simplified method. Both of these effects influence the factor of safety by about 8 percent. It should be noted that if the materials involved in the slide have a linear failure envelope, an underestimated factor of safety will be calculated if Bishop's or Janbu's simplified methods are used and the shear resistance along the vertical sides of the sliding mass is ignored. This underestimation is approximately 21 percent for the slope model presented.

Influence of Shear Strength

The results in Figure 6 are based on a ratio of friction angles for the upper (30°) and lower (8°) materials, ϕ_{up}/ϕ_l, of 3.75. Additional ratios of ϕ_{up}/ϕ_l, e.g., 1, 1.5, 3, and 3.75, were used to investigate the influence of various friction angle ratios on the 3D/2D FS ratio values. To obtain these lower ratios of ϕ_{up}/ϕ_l, the friction angle of the lower material was increased. The friction angle of the upper material remained 30 degrees so the back scarp would remain inclined at 60° and thus simulate an active pressure condition as previously discussed. It was assumed that the value of unit weight of the lower material was 18 kN/m^3 and did not vary with ϕ_l. Figures 7 through 9 show the results of these analyses for slope inclinations of 1H:1V, 3H:1V, and 5H:1V, respectively. Each relationship shown in Figures 7 through 9 for a given W/H is the average obtained from the 3D/2D FS ratio versus ϕ_{up}/ϕ_l results obtained at H = 10 and 100 m. It can be seen from Figure 9 that varying the ratio of ϕ_{up}/ϕ_l was most pronounced for the 5H:1V slope. The effect of varying ϕ_{up}/ϕ_l decreased for increasing W/H. For example, for a 5H:1V slope (Figure 9) and a value of W/H of 10 and 1, the difference in the 3D/2D FS ratio ranged from 1.6 to 2.1, respectively, for the range of ϕ_{up}/ϕ_l ratios investigated.
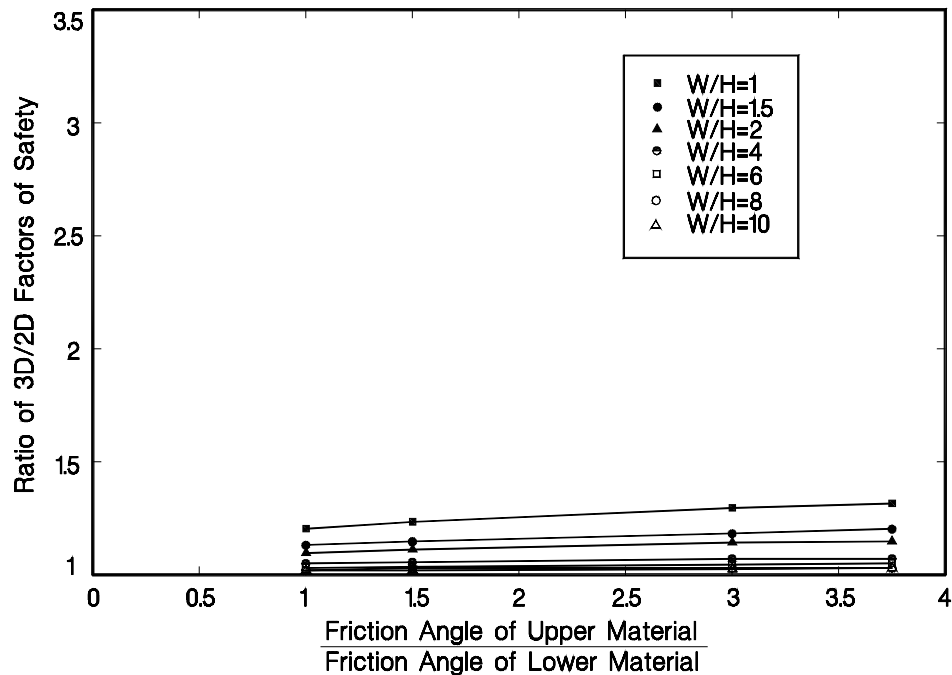

Figure 7. Influence of Shear Strength on Ratio of 3D/2D Factors of Safety for 1H:1V Slope
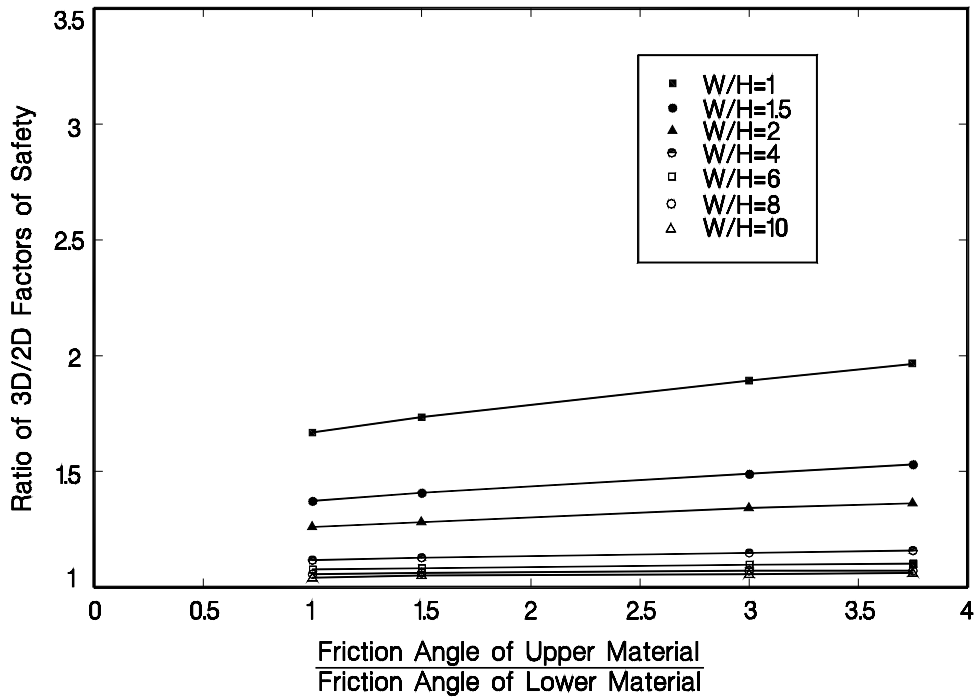
Figure 8. Influence of Shear Strength on Ratio of 3D/2D Factors of Safety for 3H:1V Slope
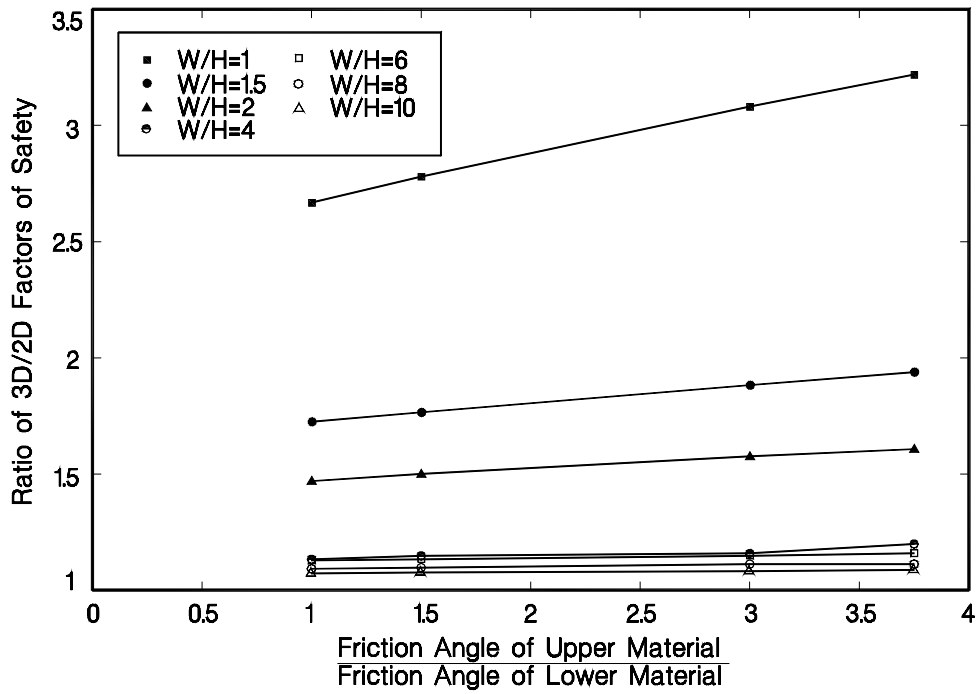

Figure 9. Influence of Shear Strength on Ratio of 3D/2D Factors of Safety for 5H:1V Slope

14

Figures 7 through 9 also show that for a given W/H ratio and back scarp angle, the influence of shear strength between the upper and lower layers increases with decreasing slope inclination. For a W/H of 1.0, back scarp angle of 60°, and a ϕ_{up}/ϕ_l of 3.75, the 3D/2D FS ratio increased from 1.31 to 3.18 for slopes of 1H:1V (Figure 7) to 5H:1V (Figure 9), respectively. For flatter slopes at a given W/H and back scarp angle, the L/H increases. Thus, the flatter slope yields a larger value of L and a larger shear stress is mobilized along the base of the sliding surface. In the previous section, it was shown that the influence of incorporating end effects in a slope stability analysis increases with decreasing slope inclination for a given W/H Ratio (see Figure 6). The results of Figures 7 through 9 indicate that this influence may become more substantial with larger differences in shear strength between upper and lower layers. Thus, in relatively flat slopes with large differences in in-situ material shear strengths, the back-calculated shear strengths may be too high or unconservative. This is especially true in translational failures that occur in relatively flat slopes where the underlying material(s) may be much weaker than the upper materials.

Figures 10 and 11 illustrate the influence of ϕ_{up}/ϕ_l on the 2D and the 3D factors of safety, respectively, instead of using a FS ratio. These figures indicate that the effect of varying the friction angle between the upper and lower layers is more significant on the 3D factor of safety than the 2D FS value. The results of Figures 10 and 11 indicate that the 3D/2D FS ratio differences obtained in Figures 7 through 9 are due primarily to changes in the 3D factor of safety rather than to changes in the 2D factor of safety. Therefore, it is even more important that material shear strength parameters are adequately defined for a 3D analysis than a 2D analyses.
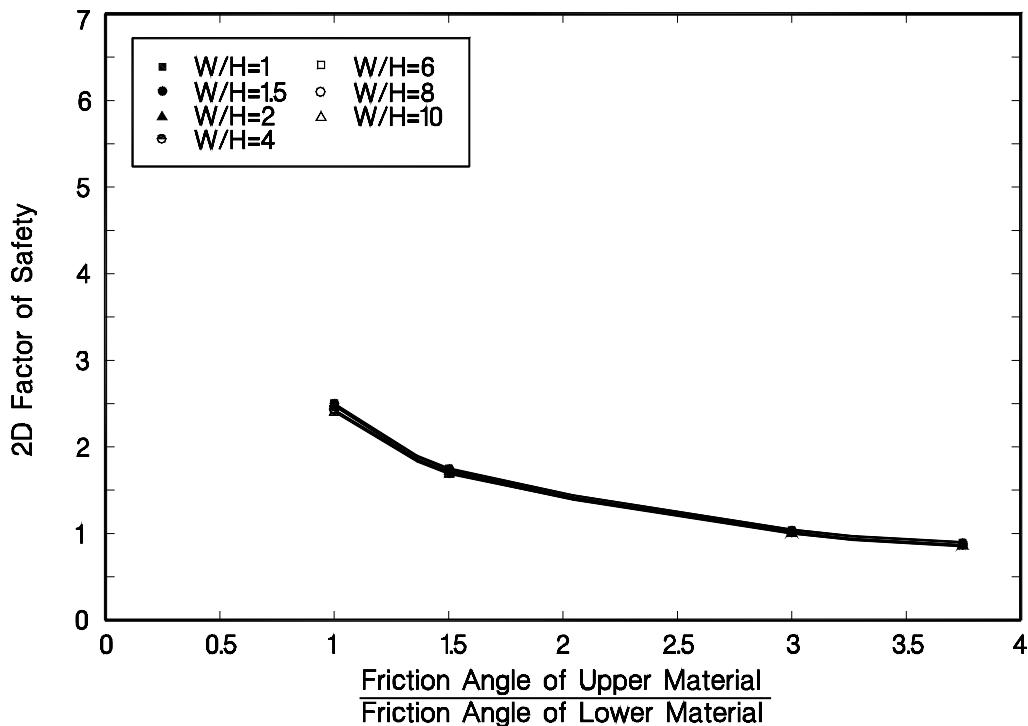

Figure 10. Influence of Shear Strength on 2D Factor of Safety for 5H:1V Slope
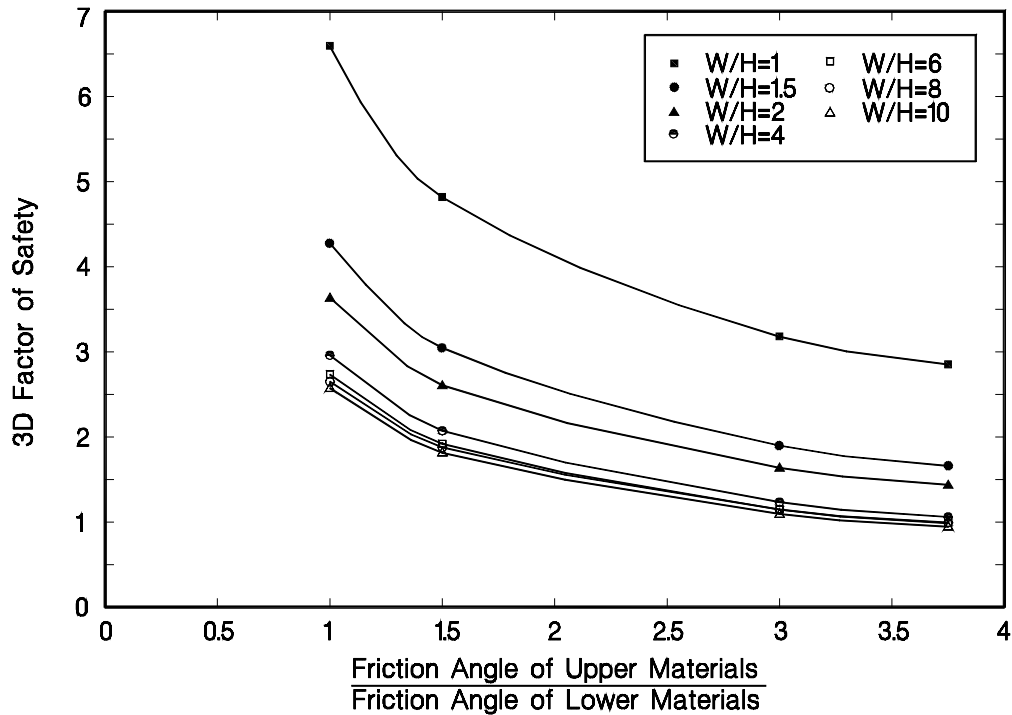
Figure 11. Influence of Shear Strength on 3D Factor of Safety for 5H:1V Slope

This parametric study was performed based on the assumption that materials along the vertical sides of the slide mass consist of cohesionless materials, i.e., cohesion, c=0. Previous studies have indicated that the 3D end effects are more pronounced for slopes of cohesive materials (Chen 1981; Lovell 1984; Leshchinsky and Baker 1986; Ugai 1988).

FIELD CASE HISTORIES

The remainder of the paper presents three field case histories that illustrate the importance of performing a 3-D slope stability analysis for remedial measures of failed slopes and the design of new slopes. Case histories of failed slopes were analyzed after the previously described slope model analysis to ensure that the findings of the parametric study represent field behavior. In addition, the failed slopes have a well defined failure surface for which the minimum 3-D factor of safety is known and equal to unity. Therefore, the minimum 3-D and 2-D factors of safety can be calculated and compared. It should be noted that a comparison between 3-D and 2-D factors of safety for a particular slope is only meaningful when the minimum factors of safety are compared (Cavounidis 1987). The parameters that were studied in the analysis of the hypothetical slope model are considered in the analysis of the field case histories. The case histories utilized English units, and thus English units are used in the text and figures with metric equivalents presented in parentheses.

San Diego Landslide

The 1979 Oceanside Manor landslide occurred along a bluff approximately 65 feet (20 m) high in a residential area in San Diego county, California. The length of the scarp is approximately 430 feet (130 m) and the slide encompassed approximately 160,000 cubic yards (122,000 m^3) of soil. Figures 12 and 13 show a plan view and a representative cross section of the landslide, respectively, prior to failure. The slope is underlain by the Santiago Formation. At this site, the Santiago Formation is composed of a claystone and a sandstone. The sandstone is fine to medium grained and overlies the gray claystone. The remolded claystone classifies as a clay or siltyclay of high plasticity, CH-MH, according to the Unified Soil Classification System. The liquid limit, plasticity index, and clay-size fraction are 89, 45, and 57 percent, respectively (Stark and Eid 1992).
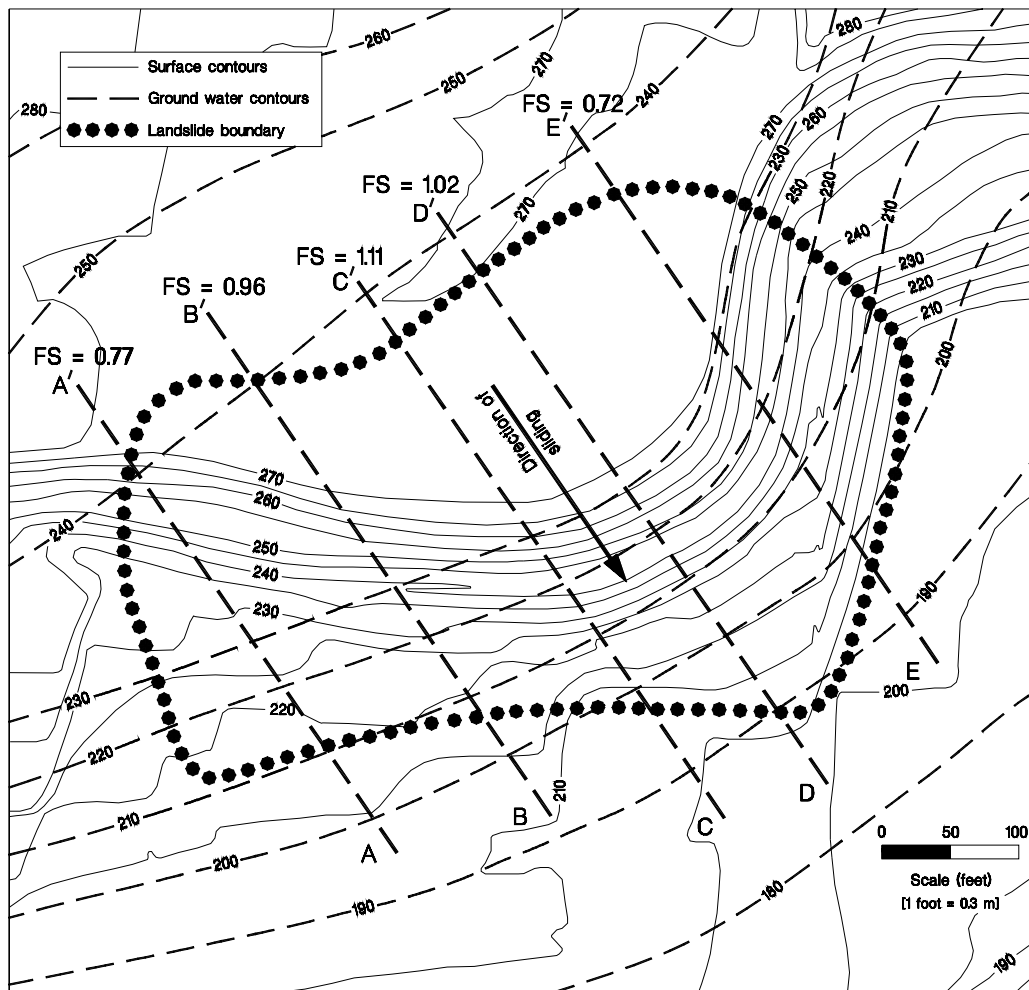

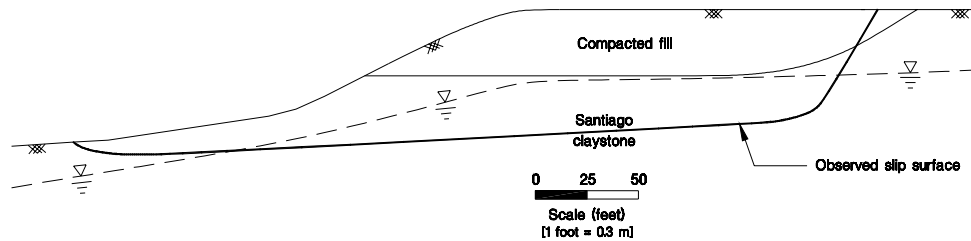**Figure 12.** Plan View of San Diego Landslide.

Figure 13. Cross Section and 2D Failure Surface of San Diego Landslide (Section D-D').

Field investigation showed that the claystone is commonly fissured, displaying numerous slickensided surfaces. The site has undergone at least three episodes of land sliding prior to the slide that is back-calculated in this paper. Therefore, the claystone has undergone substantial shear displacement and has probably reached a residual strength condition along the base of the sliding surface. In addition, the largest portion of the sliding surface in the claystone is approximately horizontal through the Santiago Formation. This indicates that sliding occurred along a weak claystone seam or layer. As a result, residual and fully softened shear strengths are assumed to be mobilized during failure along the base and the scarp in the Santiago Formation, respectively (Stark and Eid 1994, 1997). The slide surface was located using slope inclinometers and extensive borings and trenches. The ground water levels were extensively monitored using piezometers and water levels in borings and trenches shortly after movement started to occur. This resulted in the ground water contours shown in Figure 12.

A three-dimensional slope stability analysis was conducted for the sliding mass shown in Figure 14. The sides of the sliding mass were assumed to be nearly vertical. In addition, the back scarp was taken to be inclined 60 degrees from the horizontal to simulate an active earth pressure condition. The above sliding surface geometry conditions lead to a minimum sliding resistance which is expected to occur during slope failure. The moist unit weight of Santiago claystone and the compacted fill were measured to be 125 pcf (19.6 kN/m^3). Residual and fully softened shear strengths of the Santiago claystone were measured using the ring shear test procedure described by Stark and Eid (1993 and 1997), respectively. The resulting residual and fully softened failure envelopes were approximated by linear failure envelopes that pass through the origin and the average effective normal stress acting on the sliding mass base and sides, respectively. This leads to an average residual friction angle of 7.5 degrees and an average fully softened friction angle of 22.5 degrees. It should be noted that the fully softened friction angle of the claystone along the back scarp was used for calculating the mobilized shear strength of the sliding mass. The fully softened friction angle was taken to be 25 degrees (2.5 degrees higher than the value measured using the ring shear apparatus) to account for the triaxial compression mode of failure instead of the ring shear failure mode (Stark and Eid 1997). The
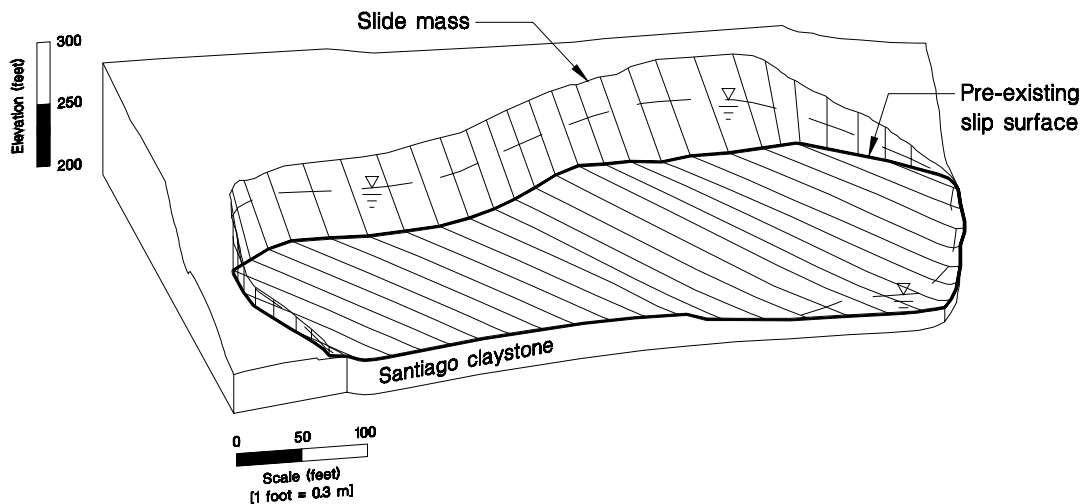
18

Figure 14. 3D View of Slide Mass for San Diego Landslide.

cohesion and friction angle of the compacted fill were measured using direct shear tests to be zero and 26 degrees, respectively.

For the sliding mass shown in Figure 14, a 3-D slope stability analysis using Janbu's simplified method yields a factor of safety of 0.94. The side resistance along the sides of the slide mass was not considered by CLARA 2.31 software in this calculated factor of safety. This 3-D factor of safety is slightly higher than the average of 2-D factors of safety of 0.92 which was calculated for 44 different cross-sections in the direction of movement through the sliding mass. The location and factor of safety for five representative cross-sections are shown in Figure 12. As discussed before, if side resistance is not included, the calculated 3-D factor of safety is close to the average of 2-D factor of safety for representative cross-sections. It should also be noted that the calculated factor of safety of 0.94 is less than a factor of safety of unity that is expected for slope at a state of incipient failure.

For the representative 2-D cross-sections, overestimating the factor of safety due to ignoring the nonlinearity of the failure envelopes approximately cancels the underestimation of the factor of safety due to using Janbu's simplified method. As a result, the main source of error in calculating the 3-D factor of safety for this case is ignoring the shear resistance along the vertical sides. The slope was reanalyzed to include the shear resistance along the vertical sides of the slide mass using the technique described previously. The coefficient of earth pressure and the friction angle used in calculating the cohesion of the imaginary layer in Equation (2) are 0.58 and 25 degrees, respectively. The reanalysis yields a 3-D factor of safety of 1.02. This represents about a 9 percent increase in the calculated 3-D factor of safety due to the side resistance. This increase is significant considering the relatively small area of

19

the vertical sides of the sliding mass (Figure 14). However, the large difference between the mobilized friction angle along the base of the slide mass and vertical sides enhanced the effect of the side resistance on the overall calculated 3-D factor of safety.

The 2-D factors of safety vary significantly according to the cross-section location because of the variations in topography and ground water level over the sliding area (Figure 12). Clearly a 3-D analysis can accommodate variations in geometry, pore-water pressure, and material properties across a site more directly than 2-D analyses. In addition, the ratio between the minimum 3-D and 2-D factors of safety is approximately 1.6. In summary, the 3-D analysis provides a meaningful technique for investigating the stability of slopes with site conditions similar to those in this case history.

This case history is used to demonstrate the use of the results of the parametric study (Figures 7 through 9). The slope had an average slope inclination of 3.5H:1V prior to failure. The W/H ratio is 130 m/20 m or 6.5. The ϕ_{up}/ϕ_l ratio (25 degrees divided by 7.5 degrees) is 3.3. Using Figure 8, a W/H of 6.5, and $\phi_{up}/\phi_l = 3.3$, a 3D/2D ratio of 1.09 is obtained for a slope of 3H:1V. Similarly, from Figure 9, a 3D/2D FS ratio of 1.14 is obtained for a slope of 5H:1V. For the landslide slope inclination of 3.5H:1V, a 3D/2D FS ratio of 1.1 can be interpolated from Figures 8 and 9. Based on the average 2D factor of safety of 0.92 from 44 different cross-sections reported by Stark and Eid (1998), the 3D factor of safety can be estimated to be 1.01 using the 3D/2D FS ratio of 1.1 from Figures 8 and 9. This estimated 3D factor of safety is in agreement with the 3D factor of safety value of 1.02 calculated by Stark and Eid (1998).

The slope inclinations in Figures 6 through 11 represent an average inclination across the landslide. Additionally, the 2D value represented by the 3D/2D FS ratios in Figures 6 through 10 is an average 2D factor of safety value across the landslide in the direction of movement. The ratio between the 3D factor of safety and the minimum 2D factor of safety may be slightly larger in practice due to the simplified model. For the Oceanside Manor case history the ratio between the 3D factor of safety and minimum 2D factor of safety is 1.6 (Stark and Eid 1998).

In summary, Figures 7 through 9 can be used to determine the importance or necessity of performing a 3D slope stability analysis for a translational failure mode in practice. However, these figures should not be used as a substitute for performing an actual 3D slope stability analysis with site specific geometry, pore-water pressure condition, and material properties.

Cincinnati Landfill Failure

On March 9, 1996, the largest slope failure in a United States municipal solid waste landfill -based on volume of waste involved - occurred approximately 9 miles (15.3 km) northeast of Cincinnati, Ohio. Figure 15 is an aerial view of the waste slide, which involved approximately 1.5 million cubic yards (1.1 million m^3) of waste and developed through the natural soil underlying 350 feet (107 m) of waste.
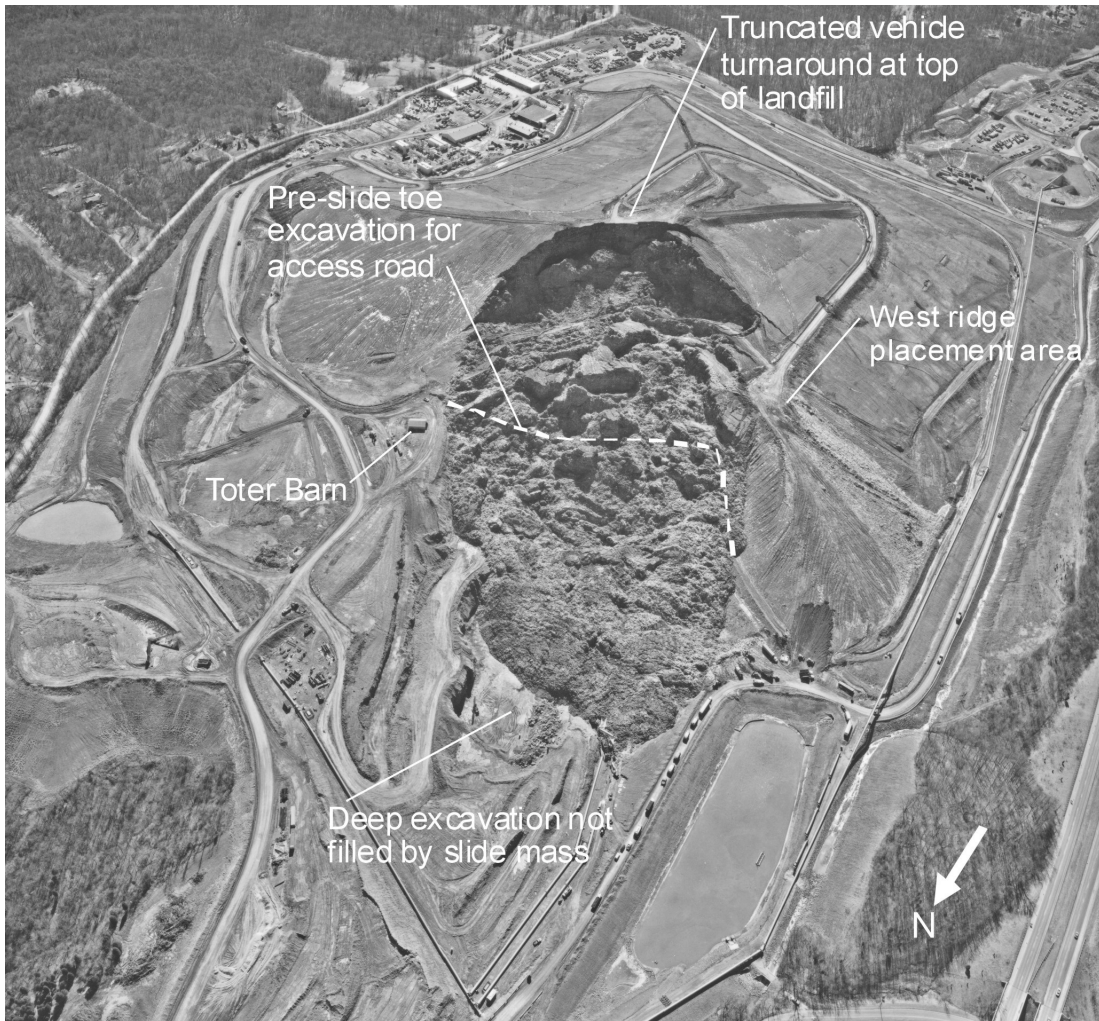
Figure 15. Aerial View of Cincinnati Landfill Failure.

Figure 16 shows a plan view of the site showing the borders of the sliding mass. The contour lines of the original ground, which consists of approximately 10 feet (3 m) of soil underlain by bedrock, and the surface of waste prior to failure are also shown in Figure 16. Stark et al. (1998) showed that the main causes for the slide are the excavation of 140 feet (42.7 m) at the toe of the existing unlined landfill to install a composite liner system, mobilizing a post-peak shear strength in the natural soil underlying the waste, overbuilding the slope by approximately one million cubic yards, and exceeding the maximum permitted elevation by approximately 50 feet (15 m).
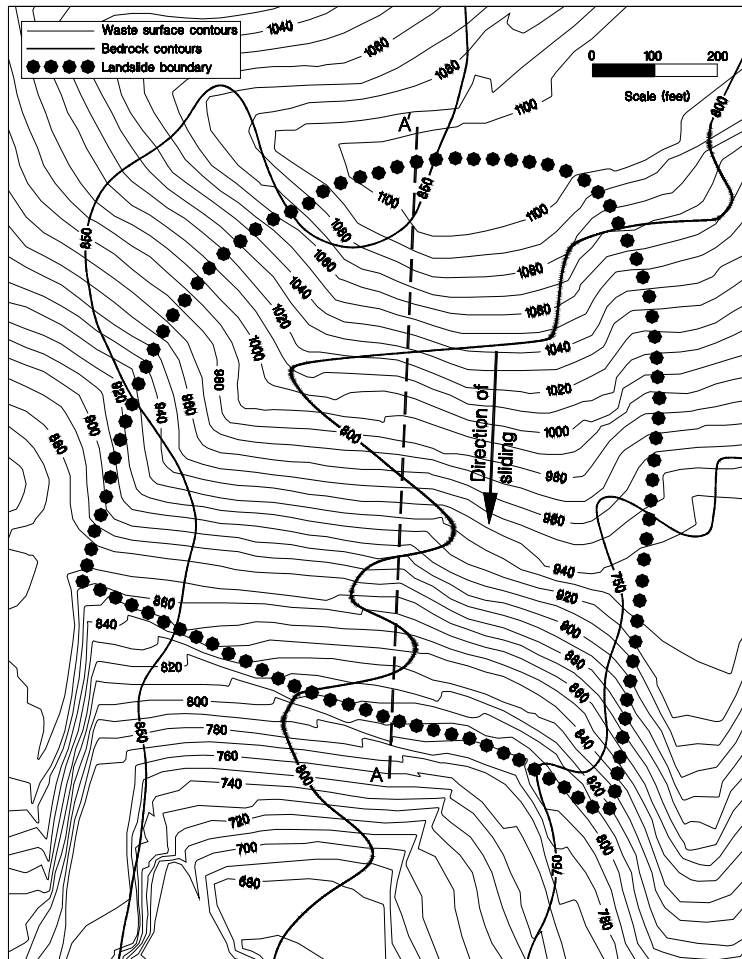
Figure 16. Plan View of Cincinnati Landfill Failure.

Field observations show that the slope began to move as a large, single slide block towards the deep excavation. As the block moved, a graben formed just behind the slide block, and an approximately 100-foot (30 m)-high scarp was created behind the graben. The formation of a large slide block, graben, and vertical scarp is indicative of a translatory landslide. Based on field observations and the results of the subsurface investigation, the failure surface was estimated to have passed through the solid waste at a near vertical inclination to the underlying natural soil. The failure surface remained in the natural soil, until it daylighted at the vertical face of the excavation at the toe of the slope (Figure 17).
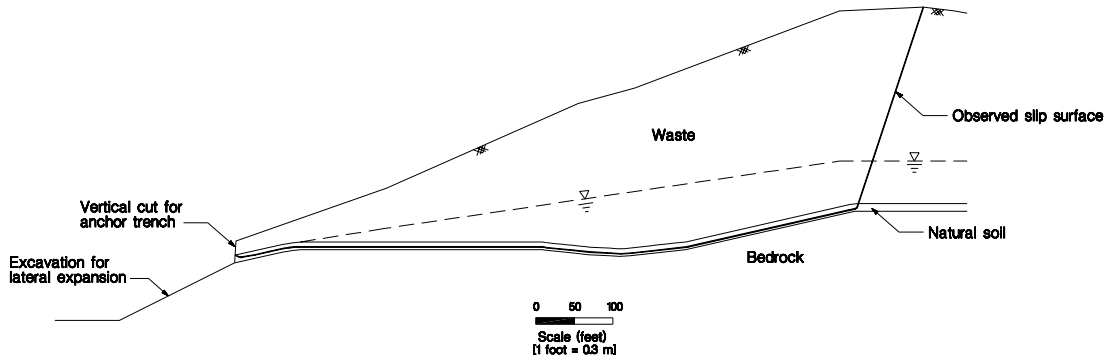
Figure 17. Cross Section and 2D Failure Surface of Cincinnati Landfill Failure (Section A-A′).

Determining the mobilized shear strength of the natural soil in this case was important for design of the reconstructed slope and the design of other interim and permanent slopes that involve a similar type of soil. Stark et al. (1998), using published data from large direct shear box testing, other case histories, the height of the vertical back scarp, and active earth pressure theory, estimated the cohesion and friction angle of the solid waste to be 845 psf (41 kPa) and 35 degrees, respectively. Moist unit weight of the solid waste was estimated to be 65 pcf (10.2 kN/m^3). To back-calculate the mobilized friction angle of the natural soil, a 3-D slope stability analysis was performed using the slope geometry shown in Figure 18 and a cohesion of zero for the natural soil. Shear resistance along the vertical sides was considered using the same technique described before. The cohesion for the imaginary layer was calculated as follows:

$$c_i' = c' + k_o \sigma'_v \tan\phi' \tag{3}$$

where c' and ϕ' are the cohesion and friction angle of the solid waste, σ'_v is the average vertical effective stress over the depth of the sliding mass side, and k_o is the coefficient of earth pressure at rest for the solid waste ($k_o = 1 - \sin\phi'$).

Because of the large difference between the shear strength of the waste and the natural soil, analyses of representative 2-D cross-sections show that underestimation of the factor of safety due to using Janbu's simplified method exceeds overestimation of the factor of safety caused by ignoring the nonlinearity of the natural soil failure envelope by approximately 7%. Consequently, this percentage is used to increase the calculated 3-D factors of safety using Janbu's simplified method and linear failure envelopes. The results of the 3-D analysis are shown in Figure 19. It can be seen that if the side resistance is considered, the back-calculated or mobilized friction angle of the natural soil is approximately 10 degrees. This value is in agreement with the drained residual friction angle of representative
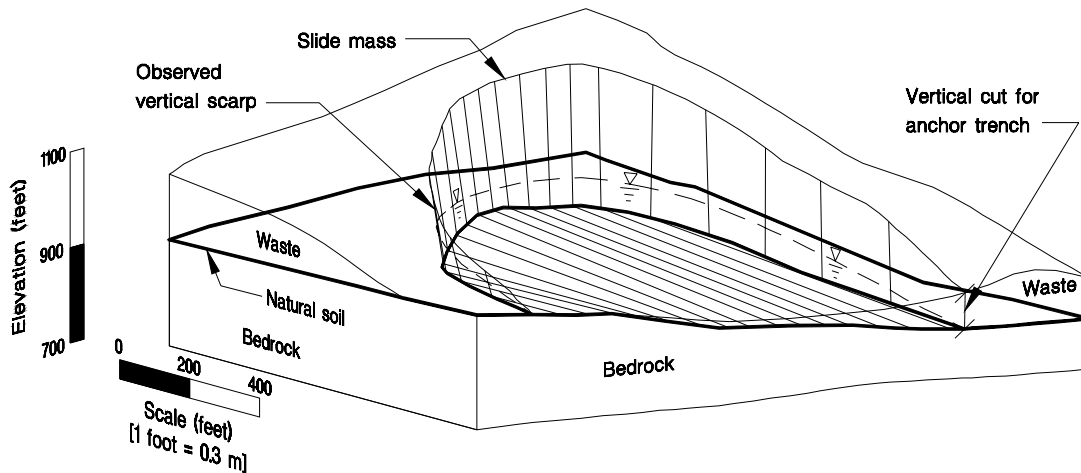
23

Figure 18. 3D View of Slide Mass for Cincinnati Landfill Failure.

samples tested using the procedure described by Stark and Eid (1993). The tested specimen has a liquid limit, plastic limit, and clay-size fraction of 69, 28, and 55 percent, respectively. A drained residual shear strength condition was probably mobilized for the natural soil in this case because of a number of reasons including the strain incompatibility between the waste and natural soil (Stark et al. 1998).

Figure 19 also shows the 3-D factors of safety and the associated back-calculated mobilized friction angles of the natural soil if the side resistance was not considered, i.e. similar to the 2-D condition. This analysis is not a true 2-D analysis because the entire slide mass is considered instead of a single cross-section. As a result, this analysis provides a factor of safety that is in between a 3-D and 2-D analysis. It can be seen that ignoring the side resistance leads to overestimation of the mobilized friction angle by approximately 30 percent. In summary, the mobilized friction angle of the natural soil estimated using a 2-D analysis of a representative cross-section would lead to an unconservative reconstructed slope. It should also be noted that if the relationship in Figure 19 that represents the 3-D analysis ignoring vertical side resistance is extended to a mobilized friction angle of zero, the calculated factor of safety would approach zero. This is because the majority of the resisting force in this analysis is derived from the shear strength along the base of the sliding mass.

The back-calculated friction angle of the natural soil is less sensitive to changes in leachate level if a 3-D analysis is used (Stark et al. 1998). The importance of the leachate level is reduced because the shear resistance along the sides of slide mass is included in the analysis. In addition, a 3-D analysis is able to accommodate a complicated leachate surface, i.e., pore pressure distribution, such as that shown in Figure 18 where the natural ground surface varies because of sloping bedrock.
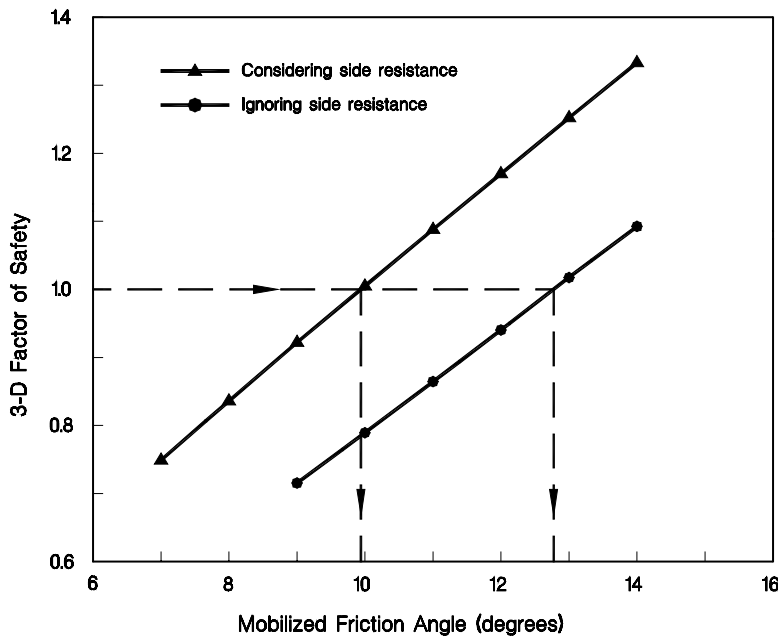
24

Figure 19. Mobilized Friction Angle and Associated 3D Factors of Safety for Cincinnati Landfill Failure.

Southern California Landfill Expansion

This case history involves some slope stability calculations for a proposed expansion of an existing landfill in southern California. The case clearly shows the importance of using a 3-D slope stability analysis in determining the critical direction of movement, i.e. the direction that yields the minimum factor of safety, for slopes with a complicated topography. The case also illustrated that 2-D factors of safety can be misleading for a well designed slope when 3-D kinematics are not incorporated.

Figure 20 is a plan view of the site showing the contour lines of the existing liner as well as the proposed waste surface. The potential scarp of the critical failure mass is also shown in Figure 20. It should be noticed that the waste rests on two different types of liners; a compacted clay liner towards the west and a geosynthetic composite liner system towards the east. The border between these two liner types is shown in Figure 20 as a heavy dashed line. Figure 21 is an aerial photograph showing the geosynthetic lined area (white) before waste placement and the existing landfill (see vehicles west of geosynthetic area). It can also be seen from Figure 20 that the compacted clay liner area, geosynthetic liner area, and the waste surface have different dip angles and directions. This difference in dip angle and direction, in addition to the existence of two different liner types at the base, makes a meaningful 2-D slope stability analysis difficult because all of these important factors cannot be incorporated into a single 2-D cross-section.
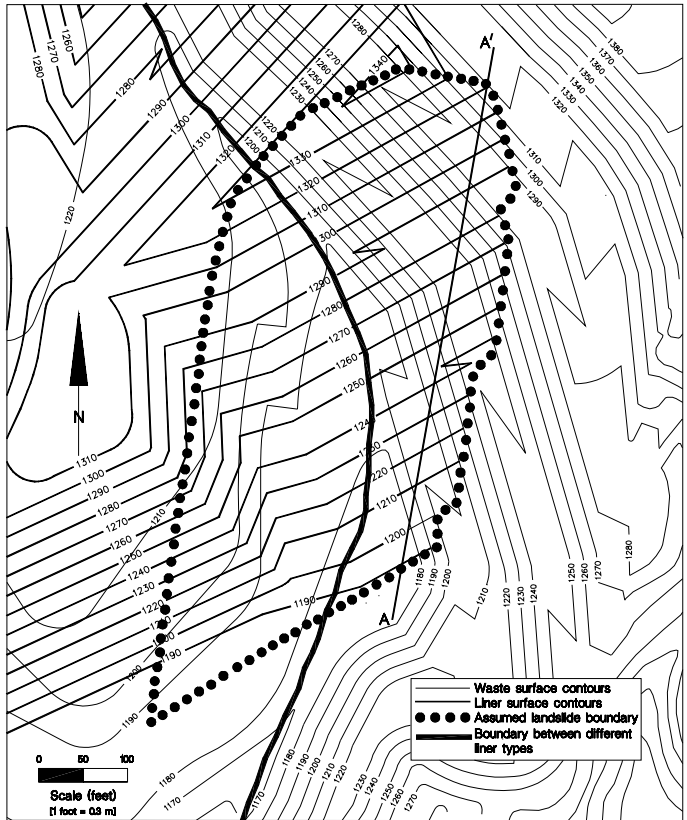
Figure 20. Plan View for California Landfill Expansion.

Figure 21. Aerial View of California Landfill Expansion with Geosynthetic Lined Area Shown in White and Existing Landfill Directly West; Note Vehicles on Existing Landfill (Photo Courtesy of Damon Brown, EBA Wastechnologies, Inc.)
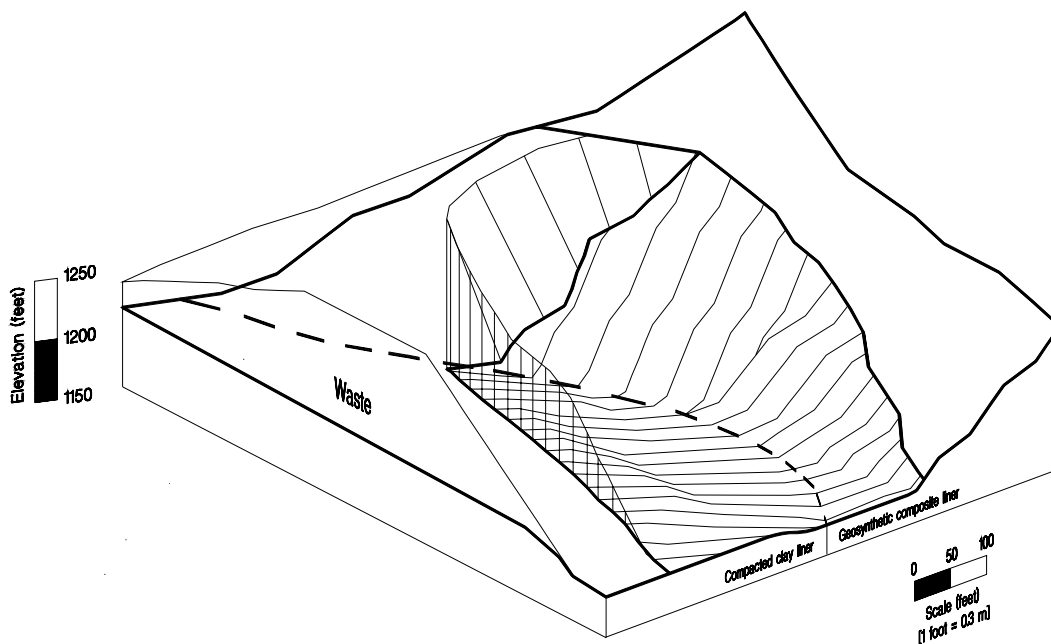
Figure 22. 3D View of Assumed Sliding Mass for California Landfill.

A three-dimensional analysis was performed using the assumed sliding mass geometry shown in Figure 22 to estimate the minimum factor of safety. It should be noticed that the waste surface meets the liner level along the east side of the sliding mass. As a result, the west side provides the largest contribution to the sliding resistance. The moist unit weight, cohesion, and friction angle of the waste were taken to be 65 pcf (10.2 kN/m^3), 104 psf (5.0 kPa), and 35 degrees, respectively. These values of the waste shear strength parameters represent the lower limit of the waste shear strength band introduced by Stark et al. (1998) so they are considered to be conservative. Since the assumed value of the waste cohesion is small, the back scarp was taken to be inclined at 60 degrees from the horizontal to simulate the active earth pressure mode. The shear resistance along the vertical side through the waste was included in the 3-D analysis using the same technique described previously. A cohesion and friction angle of 268 psf (12.8 kPa) and 19 degrees, respectively, for the compacted clay liner, and zero and 13 degrees, respectively, for the critical interface in the geosynthetic composite liner, were measured in the laboratory and used in the slope stability analysis.

Figure 23 shows the results of a search for the direction of sliding that yields the minimum 3-D factor of safety. It can be seen that a minimum factor of safety of 1.83 occurs at a direction of 26 degrees clockwise from the south direction. This direction probably reflects a weighted average between the different base dip angles and directions with their associated areas and shear strengths, and the potential failure surface. A 2-D slope stability analysis can not consider the combined effect of these factors. As a result, a 3-D analysis should be used to analyze the stability of slopes with complicated topography and site conditions similar to those in this case.
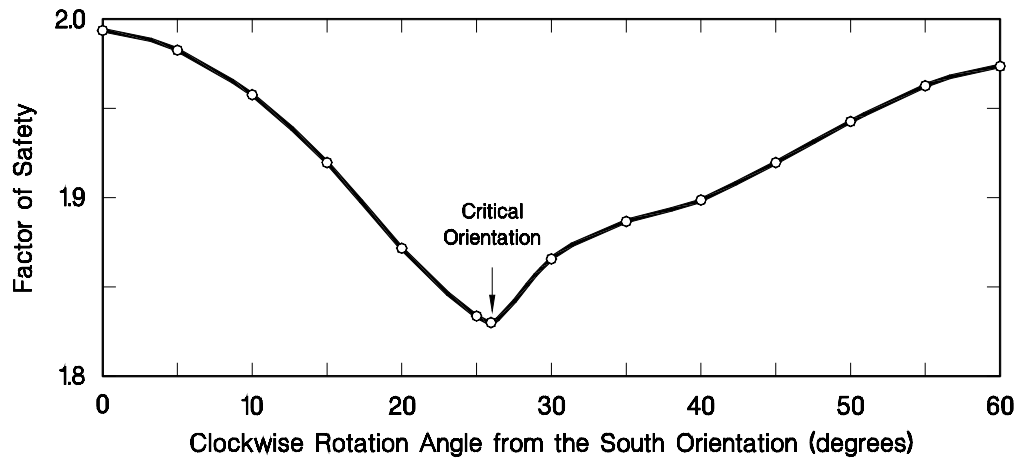
27

Figure 23. Search for Critical Sliding Direction.

Smaller sliding masses were also considered during the analysis of this landfill expansion. An example of these masses is the one that is in between cross-section A-A′ and the eastern limit of waste in Figure 20. This slide mass was thought to be critical because of the lack of sliding resistance along the east side and theresulting 2-D factor of safety of 0.97 for this cross-section. However, a 3-D analysis for sliding in the direction of cross-section A-A′ yielded a factor of safety of 1.65 for this slide mass. The high 3-D factor of safety was attributed to including the shear resistance along a vertical surface through the waste at the west side of the potential slide mass. This also emphasizes the importance of considering the 3-D behavior in slope stability analyses involving materials that exhibit a large difference in shear strength.

CONCLUSIONS

The following conclusions are based on two and three-dimensional slope stability analyses of field case histories and a representative slope model:

1.) Sides of sliding masses in translational failures are usually vertical which leads to a minimum amount of shear resistance being mobilized along these sides. However, the difference between 2-D and 3-D factors of safety is most pronounced in cases that involve a translational failure mode through low shear strength materials underlying the slide mass.

2.) Commercially available 3-D slope stability software have some limitations that affect the calculated factor of safety for a translational failure mode. These limitations include ignoring the shear resistance along the vertical sides of the sliding mass, modeling a nonlinear failure envelope with a linear failure envelope, and using a 3-D slope stability method that ignores some of the

internal shear forces. A technique is presented to overcome some of these limitations and provide a better estimate of the 3-D factor of safety.

3.) While a 3-D factor of safety is underestimated by ignoring the shear resistance along vertical sides of the slide mass, as well as the internal shear forces of the sliding mass, it is overestimated when a linear failure envelope passing through the origin and the shear strength corresponding to the average normal stress on the slip surface is used to represent a stress dependent shear strength. Underestimation of the 3-D factor of safety is maximized if the materials along the failure surface exhibit a linear failure envelope. This may lead to overestimation of the back-calculated shear strength of the materials involved in a slope failure. The difference between the 2-D and 3-D back-calculated friction angle depends on the shear strength properties of the involved materials and geometry of the sliding mass. However, this study shows that the difference in the 2-D and 3-D back-calculated friction angles can be as large as 30 percent.

4.) If the resistance along the vertical sides of the slide mass is not considered in the analysis of a translational slope failure, the calculated 3-D factor of safety will be close to the average 2-D factor of safety for representative cross-sections in the direction of movement. Therefore, it may be concluded that the 3-D factor of safety will be greater than the 2-D value for a suitable comparison.

5.) A three-dimensional analysis is beneficial in designing slopes with a complicated topography, shear strength, and/or pore-water pressure condition. For these cases, determining the direction of movement that leads to a minimum factor of safety and estimating the value of this factor requires combining the effects of slope geometry and shear strength. This can be accomplished using a 3-D analysis.

ACKNOWLEDGMENTS

REFERENCES

Baligh, M.M. and Azzouz, A.S. (1975). "End Effects of Stability of Cohesive Slopes." Journal of the Geotechnical Engineering Division, ASCE, Vol. 101, No. GT11, pp. 1105-1117.

Beene, R. R. W. (1967). "Waco Dam Slide." Journal of Soil Mechanics and Foundations Division, ASCE, Vol. 93, No. 4, pp. 35-44.

Bishop, A.W. (1955). "The Use of the Slip Circle in the Stability Analysis of Slopes," Geotechnique, Vol. 5, No. 1, pp. 7-17.

Byrne, R .J., Kendall, J., and Brown, S. (1992). "Cause and Mechanism of Failure, Kettleman Hills Landfill B-19, Unit IA" Proceedings of Stability and Performance of Slopes and Embankments-II, ASCE, Vol. 2, pp. 1188-1215.

Cavounidis, C. (1987). "On the Ratio of Factors of Safety in Slope Stability Analysis." Geotechnique, Vol. 37, No. 2, pp. 207-210.

Chen, R.H. (1981). "Three-Dimensional Slope Stability Analysis." Report JHRP-81-17, Purdue University, West Lafayette, IN, USA.

Chen, R.H. and Chameau, J.-L. (1983). "Three-Dimensional Limit Equilibrium Analysis of Slopes." Geotechnique, Vol. 32, No. 1, pp. 31-40.

Ching, R. and Fredlund, D.G (1984). "Quantitative Comparison of Limit Equilibrium Methods of Slices." Proceedings of the 4th International Symposium on Landslides, Toronto, pp. 373-379.

Duncan, J.M. (1992). "State-of-the-Art: Static Stability and Deformation Analysis." Proceedings of Stability and Performance of Slopes and Embankments-II, ASCE, Vol. 1, pp. 222-266.

Ehlig, P. L. (1992). "Evolution, Mechanics and Mitigation of the Portuguese Bend Landslide, Palos Verdes Peninsula, California." Engineering Geology Practice in Southern California, B. W. Pipkin and R. J. Proctor, eds., Star Publishing Co., Belmont, Calif., pp. 531-553.

Eid, H. T. (1996). "Drained Shear Strength of Stiff Clays for Slope stability Analyses." PhD thesis, University of Illinois at Urbana-Champaign, Urbana, Illinois.

Fredlund, D. G., and Krahn, J. (1977). "Comparison of Slope Stability Methods of Analysis." Canadian Geotechnical Journal, Vol. 14, No. 3, pp. 429-439.

Gens, A., Hutchinson, J.N. and Cavounidis (1988). "Three-Dimensional Analysis of Slides in Cohesive Soils." Geotechnique, Vol. 38, No. 1, pp. 1-23.

Hoek, E., and Brown, E.T. (1980). "Underground Excavations" Institution of Mining and Metallurgy, London, England, p. 527.

Hungr, O. (1987). "An Extension of Bishop's Simplified Method of Slope Stability Analysis to Three Dimensions." Geotechnique, Vol. 37, No. 1, pp. 113-117.

Hungr, O. (1988). "CLARA: Slope Stability Analysis in Two or Three Dimensions." O. Hungr Geotechnical Research, Inc., Vancouver, B.C.

Hungr, O., Salgado, F.M. and Byrne, P.M. (1989). "Evaluation of a Three-Dimensional Method of Slope Stability Analysis." Canadian Geotechnical Journal, Vol. 26, pp. 679-686.

Janbu, N. (1968). "Slope Stability Computations." Soil Mechanics and Foundation Engineering Report, Technical University of Norway, Trondheim.

Jasper, J. L., and Peters, N. (1979). "Foundation Performance of Gardiner Dam." Canadian Geotechnical Journal, Vol. 16, pp. 758-788.

Kavazanjian, E., Matasovi, N., Bonaparte, R., and Schmertmann, G.R. (1995). "Evaluation of MSW Properties for Seismic Analysis." Proceedings of Geoenvironment 2000 Specialty Conference, ASCE, New Orleans, Vol. 2, pp. 1126-1141.

Krahn, J., Johnson, R. F., Fredlund, D. G., and Clifton, A. W. (1979). "A Highway Cut Failure in Cretaceous Sediments at Maymont, Saskatchewan" Canadian Geotechnical Journal, Vol. 16, pp. 703-715.

Leshchinsky, D., Baker, R. and Silver, M. L. (1985). "Three Dimensional Analysis of Slope Stability." International Journal for Numerical and Analytical Methods in Geomechanics, Vol. 9, No. 2, pp. 199-223.

Leshchinsky, D. and Baker, R. (1986). "Three-Dimensional Slope Stability: End Effects." Soils and Foundations, JSSMFE, Vol. 26, No. 4, pp. 98-110.

Lovell, C.W. (1984). "Three Dimensional Analysis of Landslides." Proceedings of the 4th International Symposium on Landslides, Toronto, pp. 451-455.

Pyke, R. (1991). "TSLOPE3: Users Guide." Tag a Engineering Systems and Software, Lafeyette, CA.

Seed, R.B., Mitchell, J.K. and Seed, H.B. (1990). "Kettleman Hills Waste Landfill Slope Failure. II: Stability Analysis." <u>Journal of Geotechnical Engineering</u>, ASCE, Vol. 116, No. 4, pp. 669-689.

Skempton, A. W. (1985). "Residual Strength of Clays in Landslides, Folded Strata and the Laboratory." <u>Geotechnique</u>, Vol. 35, No. 1, pp. 3-18.

Spencer, E. (1967). "A Method of Analysis of the Stability of Embankments Assuming Parallel Inter-Slice Forces." <u>Geotechnique</u>, Vol. 17, No. 1, pp. 11-26.

Stark, T.D. and Eid, H. T. (1992). "Comparison of Field and Laboratory Residual Shear Strengths." <u>Proceedings of Stability and Performance of Slopes and Embankments-II</u>, ASCE, Vol. 1, pp. 876-889.

Stark, T. D. and Eid, H. T. (1993). "Modified Bromhead Ring Shear Apparatus." <u>ASTM Geotechnical Journal</u>, Vol. 16, No. 1, pp. 100-107.

Stark, T. D., and Eid, H. T. (1994). "Drained Residual Strength of Cohesive Soils." <u>Journal of Geotechnical Engineering</u>, ASCE, Vol. 120, No. 5, pp. 856-871.

Stark, T.D. and Poeppel, A.R. (1994). "Landfill Liner Interface Strengths from Torsional Ring Shear Tests." <u>Journal of Geotechnical Engineering</u>, ASCE, Vol. 120, No. 3, pp. 597-615.

Stark, T. D., Williamson, T. A., and Eid, H. T. (1996). "HDPE Geomembrane/Geotextile Interface Shear Strength." <u>Journal of Geotechnical Engineering</u>, ASCE, Vol. 122, No. 3, pp. 197-203.

Stark, T. D., and Eid, H. T. (1997). "Slope Stability Analyses in Stiff Fissured Clays." <u>Journal of Geotechnical and Geoenvironmental Engineering</u>, ASCE, Vol. 123, No. 4, pp. 335-343.

Stark, T. D., Eid, H. T., Evans, W. D., and Sherry, P. E. (1998). "Slope Failure in a Municipal Solid Waste Landfill." Paper accepted for publication in <u>Journal of Geotechnical and Geoenvironmental Engineering</u>, ASCE.

Thomaz, J. E. (1986). "A General Method for Three Dimensional Slope Stability Analysis." Information Report, Purdue University, West Lafayette, IN.

Thomaz, J. E., and Lovell, C.W. (1988). "Three Dimensional Slope Stability Analysis with Random Generation of Surfaces." <u>Proceedings of the 5th International Symposium on Landslides</u>, Lausanne, Vol. 1, pp. 777-781.

Ugai, K. (1988). "Three-Dimensional Slope Stability Analysis by Slice Methods." Proceedings of the 6th International Conference on Numerical Methods in Geomechanics, Innsbruck, pp. 1369-1374.

Wright, S. G., and Duncan, J. M. (1972). "Analyses of Waco Dam Slide." Journal of Soil Mechanics and Foundations Division, ASCE, Vol. 98, No. 9, pp. 869-877.

Wright, S. G. (1992). "UTEXAS3: A Computer Program for Slope Stability Calculations." Geotechnical Engineering Software GS86-1, Department of Civil Engineering, University of Texas, Austin, pp. 109.